Nonequilibrium self-organization phenomena in active Langmuir monolayers

Tatsuo Shibata
Department of Mathematical and Life Sciences, Hiroshima University, 1-3-1, Kagamiyama, Higashi-Hiroshima, 739-8526, Japan

Alexander S. Mikhailov
Abteilung Physikalische Chemie, Fritz-Haber-Institut der Max-Planck-Gesellschaft, Faradayweg 4-6, 14195 Berlin, Germany

Langmuir monomolecular layers, formed by amphiphilic molecules at liquid-air interfaces and containing a fraction of chiral molecules, are theoretically investigated. These monolayers can be brought out of thermal equilibrium by applying a gradient of small molecules across the interface, resulting in the leakage flow. We show that, when splay coupling between the orientation field and the local concentration of chiral molecules in the monolayer is taken into account, this nonequilibrium soft matter system can show complex wave behavior, including the development of target wave patterns, spiral waves, and dense regions filled with inwardly propagating waves. © *2006 American Institute of Physics*. [DOI: 10.1063/1.2213580]

Nonequilibrium soft matter can show various phenomena of self-organization based on the interplay between reactions, diffusion, and phase transitions.[1] These self-organization processes are essential for the operation of biological cells[2,3] and can find potential applications in the artificial nanodevices based on soft nanotechnologies. An important difference between reaction-diffusion systems and the reactive soft matter is that, instead of forming concentration patterns, soft-matter systems are building physical structures characterized by cohesion. In contrast to propagating concentration waves, traveling structures in these systems are accompanied by real material transport and structural changes. While some kinds of soft matter, including macromolecules and biomembranes, are complex, there are also systems with a simpler organization where similar effects can be observed. An example of an inorganic soft matter is provided by monomolecular adsorbate layers on metal surfaces, where structural phase transitions inside the monolayers or in the underlying metal substrate can be coupled with chemical reactions.[4,5] In this article, we discuss self-organization phenomena in a different type of monomolecular films, i.e., in the Langmuir monolayers formed by organic lipid or amphiphilic molecules at water-air interfaces. The Langmuir monolayers bear strong similarity to biomembranes, representing lipid bilayers. However, they always remain strictly planar and the effects of curvature and shape changes are not involved in such systems.

I. INTRODUCTION

At thermal equilibrium, Langmuir monolayers are characterized by a variety of phase transitions which are accompanied by the emergence of orientational and translational order.[6] Langmuir monolayers, formed by a mixture of two components, may undergo phase separation and spontaneous formation of surface domains rich in one of the two components. To bring such monolayers far from equilibrium, various methods can be employed. By illuminating them with the light of a particular wavelength, transitions between different conformational states of organic molecules can be induced, leading to the development of traveling wave structures.[7,8] Theoretical analysis of photoinduced traveling structures in such nonequilibrium two-component monolayers has been performed.[9–11]

More recently, another, very elegant, method of inducing nonequilibrium self-organization in Langmuir monolayers containing chiral molecules has been proposed. In the experiments of Tabe and Yokoyama,[12] the monolayers were placed at an interface between glycerol and air. The glycerol also contained, however, some water molecules that could leak into the air by passing through the interfacial monolayer. Each chiral molecule can be viewed as a miniature propeller that may start to rotate powered by the leakage flow of small water molecules crossing the interface. Using reflected light polarization microscopy, these authors could show that precession of the azimuthal orientation can be induced by such leakage flows. The observed precession frequency was directly proportional to the gradient of water molecules across the monolayer, i.e., to the difference of their concentrations in the air and glycerol; the precession direction (counterclockwise or clockwise) was reversed when the vapor concentration in the air was high and water molecules were going into the glycerol from the air. Remarkably, such orientational oscillations were always accompanied by the formation of some wave patterns. Typically, they included wave sources and could be described as target patterns, bearing some similarity to the target patterns in the Belousov-Zhabotinsky reaction.[13]

Biological membranes often include many active inclusions, such as molecular pumps, and their interactions with

the membrane may lead to rich nonequilibrium phenomena.[14,15] Protein motors, representing active molecular oscillators, can form thin planar layers where complex nonequilibrium patterns may be observed.[16,17] Conceptually, such active molecular arrays are similar to Langmuir monolayers containing chiral molecules driven by the leakage flows. Here, the active elements are not the molecular motors, whose cycles are powered by binding of ligands. Instead, active elements in such systems represent molecular rotors whose rotations are produced by the flux of small (water) molecules. It should be stressed that the observed azimuthal rotations correspond to coherent rotations of a great number of such rotors and already indicate synchronization of cyclic motions in a large population of such molecular objects.

The understanding of molecular synchronization mechanisms responsible for coherent precession of chiral molecules in Langmuir monolayers is still largely missing (see, however, a discussion of energetic aspects of this phenomenon in Ref. 12). Currently, theoretical investigations are focused on the analysis of self-organization effects underlying the formation of wave patterns in such systems. In the original publication,[12] target patterns were interpreted as arising due to the special boundary conditions: if the azimuthal orientation is pinned along the boundaries of a medium, oscillations taking place in its center should send waves propagating to the boundaries and eventually stopping there. This interpretation was also followed by Tsori and de Gennes,[18] where creation of orientational defects was additionally taken into account.

In our short publication,[19] a different explanation of experimentally observed wave patterns was suggested, where the boundaries did not play an important role and traveling waves were developing due to a splay coupling between the orientation field and the local concentration of chiral molecules. Similar splay coupling was previously used to describe spontaneous formation of equilibrium periodic stripe patterns in Langmuir monolayers.[20–23] Besides the target patterns, our theory predicts other kinds of structures, such as, e.g., rotating spiral waves. In the present article, a detailed description of the theory is provided and additional results and model extensions are reported. The model of a chiral Langmuir monolayer with splay coupling between the orientation and concentration is formulated in the next section. The equilibrium properties of this model and its linear thermodynamic responses to weak leakage fluxes are considered in Sec. III. Numerical simulations of nonequilibrium wave patterns in this system are described in Secs. IV and V. The paper ends with the conclusions and a discussion of obtained results.

II. FORMULATION OF THE MODEL

We study a model of an orientationally ordered two-component Langmuir monolayer representing a mixture of chiral and achiral molecules (in the experiments,[12] chiral molecules made up only 10% of the monolayer). The local state of the monolayer is described by the variable c, giving the local fraction of chiral molecules, and by the orientation vector $\mathbf{n}$ that represents projection of the molecular tilt onto

the monolayer plane. In our simple model, we assume that density of the monolayer is fixed. The Landau free energy of the system is

$$F = \int \left[\tfrac{1}{2}K(\nabla \mathbf{n})^2 + k_B T c \ln c + k_B T(1-c)\ln(1-c) \right.$$
$$\left. + \tfrac{1}{2}G(\nabla c)^2 + \Lambda c \nabla \cdot \mathbf{n} \right] dxdy. \quad (1)$$

The first term corresponds to the elastic energy of orientational ordering (K is the Frank elastic constant). The next two terms determine the lattice-gas entropy contribution to the free energy (T is the temperature and k_B is the Boltzmann constant), and the following term (with the coefficient G) takes into account weak energetic interactions between chiral molecules which favor their uniform spatial distribution. The last term in the expression for free energy describes splay interactions in the system. It provides coupling between the scalar concentration field c and the vector orientational field $\mathbf{n}$;[20] the parameter Λ specifies the strength of splay interactions.[24]

Assuming pure relaxational dynamics, the evolution equation for concentration c of chiral molecules is

$$\dot{c} = \frac{D}{k_B T} \nabla \left[c(1-c) \nabla \mu \right], \quad (2)$$

where D is the diffusion constant, $D/k_B T$ is the mobility of chiral molecules, and

$$\mu(\mathbf{r},t) = \frac{\delta F}{\delta c(\mathbf{r},t)} \quad (3)$$

is the local chemical potential.

The kinetic equations for the orientation field $\mathbf{n}$ are

$$\dot{n}_x = -\Gamma \frac{\delta F}{\delta n_x(\mathbf{r},t)} + \Omega n_y, \quad \dot{n}_y = -\Gamma \frac{\delta F}{\delta n_y(\mathbf{r},t)} - \Omega n_x. \quad (4)$$

In addition to the relaxation terms (Γ is the relaxation rate constant for orientational ordering), we have phenomenologically included into these equations, following Ref. 12, a term that describes planar precession of the orientation vector. This precession is caused by the leakage flow and its frequency Ω is linearly proportional to the flow intensity (as seen in the experiments in Ref. 12). Because of the flow terms, the system cannot relax to the state of thermal equilibrium, and oscillations and active wave propagation become possible.

Using expression (1) for the free energy F, rescaling time and spatial coordinates as $t \rightarrow t(k_B T\Gamma)^{-1}$ and $\mathbf{r} \rightarrow \mathbf{r}(K/k_B T)^{1/2}$, and introducing the angle variable ϕ defined by $\mathbf{n} = (\cos\phi, \sin\phi)$, kinetic equations (2) and (4) can be written in the form

$$\dot{c} = \nu\{\nabla^2 c - g \nabla [c(1-c)\nabla^3 c] + \lambda \nabla [c(1-c) \nabla(\nabla \cdot \mathbf{n})]\}, \quad (5)$$

$$\dot{\phi} = \nabla^2 \phi - \omega + \lambda \left(\cos\phi \frac{\partial c}{\partial y} - \sin\phi \frac{\partial c}{\partial x} \right). \quad (6)$$

The coefficients in these equations are $\nu = D(K\Gamma)^{-1}$, $g = GK^{-1}$, $\lambda = \Lambda/(k_B TK)^{1/2}$, and $\omega = \Omega(k_B T\Gamma)^{-1}$. Note that the total amount of chiral molecules is conserved and the aver-

age spatial concentration c_0 of these molecules is a parameter of the system. According to Eq. (5), splay coupling to the orientation field leads to physical forces acting on chiral molecules and to the viscous flow of these molecules in the monolayer plane. On the other hand, spatial gradients of concentration c lead, according to Eq. (6), to local rotation of the orientation vector **n**.

In the model (5) and (6), which has been previously considered,[19] the precession frequency ω is constant. If the local concentration c of chiral molecules shows, however, significant variations over the monolayer, this assumption should be modified. Indeed, the precession is possible only when locally the chiral molecules are present. Therefore, one can expect that the precession frequency should decrease with the concentration. For relatively small concentrations, a linear dependence $\omega = \alpha c$ can be phenomenologically chosen. Conveniently, this dependence can also be expressed as

$$\omega = \omega_0 \frac{c}{c_0}, \tag{7}$$

where ω_0 is the frequency of the uniform precession in the state with $c = c_0$.

III. EQUILIBRIUM PATTERNS

When the leakage flow is absent ($\omega = 0$), kinetic equations (5) and (6) describe relaxation to thermal equilibrium that corresponds to a minimum of the free energy (1). If splay interactions are absent ($\lambda = 0$), the equilibrium state of the system is uniform: $c = c_0$ and $\phi = \phi_0$. Increasing the intensity of splay interactions, this uniform state becomes unstable and gives rise to a spatially modulated stripe structure.

To analyze the instability of the uniform state, we introduce small perturbations $c = c_0 + \delta c$ and $\phi = \phi_0 + \delta\phi$. If they depend only on the spatial coordinate x, the evolution of these perturbations is described by the linearized kinetic equations

$$\frac{1}{\nu}\dot{\delta c} = \frac{\partial^2 \delta c}{\partial x^2} - g c_0(1-c_0)\frac{\partial^4 \delta c}{\partial x^4} - \lambda c_0(1-c_0)\sin \phi_0 \frac{\partial^3 \delta\phi}{\partial x^3}, \tag{8}$$

$$\dot{\delta\phi} = \frac{\partial^2 \delta\phi}{\partial x^2} - \lambda \sin \phi_0 \frac{\partial \delta c}{\partial x}. \tag{9}$$

The solution of these linear equations can be sought in the form $\delta c \propto \delta\phi \propto \exp(\gamma t + ikx)$. The growth rate γ of the perturbation mode with the wave number k satisfies the characteristic equation

$$\gamma^2 + k^2\gamma[1 + \nu + \nu g c_0(1-c_0)k^2]$$
$$+ \nu k^4[1 + g c_0(1-c_0)k^2 - \lambda^2 c_0(1-c_0)\sin^2 \phi_0] = 0. \tag{10}$$

The uniform state is unstable if there is an interval of wave numbers k inside which the growth rate γ is positive. A simple analysis shows that this instability is found only for sufficiently strong splay coupling, when the coupling constant $|\lambda|$ exceeds the critical value λ_{cr} given by
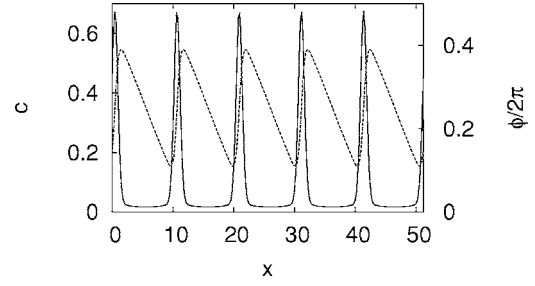

FIG. 1. Profiles of concentration c (solid) and azimuthal angle $\phi/2\pi$ (dashed) in an equilibrium stripe pattern starting from random initial conditions for the azimuthal angle field ϕ and $c = c_0$ for $c_0 = 0.1$, $\nu = 0.1$, $g = 1$, and $\lambda = 4$. The system length is $L = 51.2$.

$$\lambda_{cr} = \frac{1}{|\sin \phi_0|\sqrt{c_0(1-c_0)}}. \tag{11}$$

For $|\lambda| > \lambda_{cr}$, however, the uniform state becomes unstable with respect to growth of spatial modes with the wave numbers $0 < k < k_{max}$, where

$$k_{max}^2 = \frac{1}{g c_0(1-c_0)}\left(\frac{\lambda^2}{\lambda_{cr}^2} - 1\right). \tag{12}$$

The instability first takes place for periodic spatial modulation in the direction x orthogonal to the equilibrium orientation (i.e., for $\phi_0 = \pm \pi/2$). This instability has previously been investigated and is known to lead to the formation of an equilibrium periodic stripe pattern.[20] In this equilibrium pattern, both the local concentration and the orientation are periodically varying along a certain direction. The remarkable property of such equilibrium phase transition is that the characteristic wavelength $2\pi/k_{max}$ of the emerging periodic stationary structure diverges as $(\lambda^2 - \lambda_{cr}^2)^{-1/2}$ at the transition point. The amplitude of the periodic structure decreases as the critical point is approached and vanishes at $|\lambda| = \lambda_{cr}$.

Figure 1 shows profiles of the azimuthal angle and local concentration in the equilibrium one-dimensional periodic stripe pattern, obtained by numerical integration of the nonlinear evolution equations (5) and (6) with $\omega = 0$. Note that the angle ϕ shows only periodic modulation around a stationary level, with the modulation amplitude never exceeding 2π, so that orientation rotations do not occur in this spatial structure.

Additionally, the system always has periodic domain solutions characterized by rotations of the orientation field. In numerical simulations for a one-dimensional system of length L, they can be obtained by applying periodic boundary conditions and requiring that the $\phi(L) - \phi(0) = 2\pi n$ with $n = 1, 2, 3, \ldots$. An example of such an equilibrium domain pattern is shown in Fig. 2. Inside each domain, full 2π rotation of the azimuthal angle takes place. The angle changes steeply within relatively narrow domain boundaries. In such narrow domain boundaries, local concentration of chiral molecules becomes increased. Such periodic domain patterns are possible for any splay coupling intensities λ. When $\lambda \rightarrow 0$, spatial modulation of the concentration c gradually disappears and the spatial dependence of the angle variable ϕ becomes linear, $\phi = \phi_0 + 2\pi n x/L$.
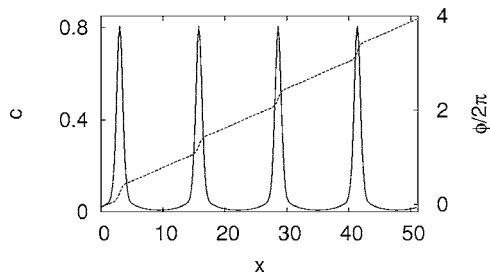
FIG. 2. Profiles of concentration c (solid) and azimuthal angle $\phi/2\pi$ (dashed) in an equilibrium domain pattern starting from an initial condition $c=c_0$ and $\phi(x)=\pi x/6.4$ for $c_0=0.1$, $\nu=0.1$, $g=1$, and $\lambda=4$. The system length is $L=51.2$.

Numerical simulations of equilibrium patterns in two-dimensional media were performed. In our simulations, the explicit Euler scheme with constant coordinate and time steps was used. Periodic boundary conditions were typically applied, to avoid boundary effects. As the initial condition, a state with the uniform concentration of chiral molecules and an orientation pattern, representing a random superposition of several spatial Fourier modes, was chosen.

Two examples of equilibrium 2D patterns in systems with different parameters are shown in Fig. 3. In both cases, the splay coupling is so strong that $\lambda>\lambda_{cr}$ and the uniform state is unstable with respect to the formation of spatial structures. These structures are much more complicated than the periodic one-dimensional structures displayed in Figs. 1 and 2. They are formed by some irregular, curved lines decorated with orthogonally oriented protrusions. Across these lines, the angle undergoes a significant change within a nar-
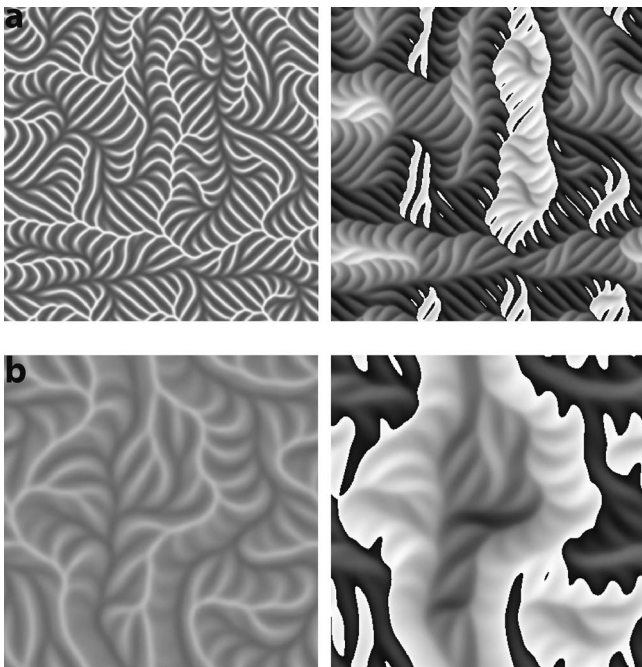

FIG. 3. Distributions of concentration (left panels) and azimuthal angle (right panels) in an equilibrium pattern obtained starting from random initial conditions for systems with the parameters $c_0=0.1$, $\lambda=4$, $\nu=10$, $\omega=0$, and $L=600$. (a) $g=10$. (b) $g=100$. The concentration is displayed in gray scale with the darker color corresponding to lower concentration values. The angle ϕ is displayed modulus 2π.
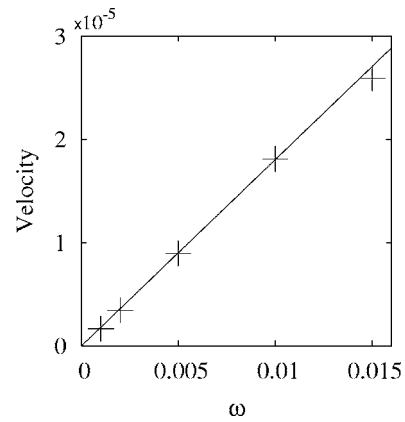

FIG. 4. Velocity dependence of a traveling stripe pattern on ω for $c_0=0.2$, $\nu=0.1$, $g=1$, and $\lambda=3$ with Eqs. (5) and (6).

row spatial interval and, moreover, the concentration of chiral molecules is much increased there. Therefore, such curved lines are similar to the domain boundaries in the one-dimensional domain structure (cf. Fig. 2). On the other hand, the angle variation across the orthogonal protrusions is not large. It can be checked that the characteristic length scale of this structure is close to the spatial period of the stripe pattern, spontaneously developing from the uniform state under the same conditions in the one-dimensional media. Therefore, such two-dimensional structures can be considered as consisting of a combination of equilibrium periodic stripe patterns and irregular orientation domains.

In Fig. 3(b), the coefficient g that characterizes energetic interactions between the molecules is increased with respect to the situation shown in Fig. 3. We see that this leads to an increase of the characteristic length scale of the patterns. This is in agreement with the analytical result (12), according to which the characteristic wavelength $2\pi/k_{max}$ of the periodic stripe patterns should increase when the coefficient g gets larger.

IV. TRAVELING 1D STRUCTURES

Application of leakage gradients brings the system away from thermal equilibrium and leads to the development of wave activity. The effects of leakage are simpler in the one-dimensional geometries, which shall be discussed in this section.

When $\omega\neq0$, traveling structures are observed in the 1D simulations. For small leakage fluxes, their instantaneous profiles of the angle and concentration variables are only slightly different from those in the respective equilibrium patterns (with $\omega=0$). By running numerical simulations, the velocities of the traveling stripe structure have been determined as a function of the parameter ω. The observed dependence of the stripe structure velocity on this parameter is displayed in Fig. 4.

We see that, with a good accuracy, this dependence is linear and there is no threshold that should be overcome in order to transform stationary domains into a traveling structure. This indicates that the transition to traveling stripes represents a linear thermodynamic response of the equilibrium
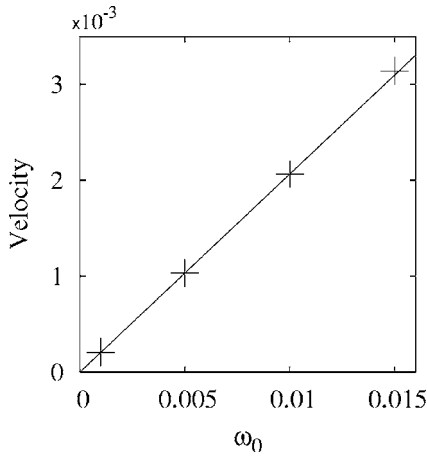
FIG. 5. Velocity dependence of a traveling stripe pattern on ω_0 for c_0 $=0.2$, $\nu=0.1$, $g=1$, and $\lambda=3$ with Eqs. (5)–(7).

FIG. 7. Velocity of a traveling domain pattern starting from an initial condition $c=c_0$ and $\phi(x)=\pi nx/12.8$ for $n=1(*),4(\bullet),8(+)$ as a function of ω_0 for Eqs. (5)–(7) with $c_0=0.1$, $\nu=0.1$, $g=1$, and $\lambda=4$.

stripe structure to the application of a weak perturbation represented by the flux terms proportional to ω in the kinetic evolution equations (5) and (6).

So far, the results of numerical simulations for the model with constant precession frequency ω have been presented. Similar results are, however, also obtained for the modified model where the frequency is proportional to the concentration of chiral molecules ($\omega=\alpha c$). The main difference is that the stripe structures move significantly faster in this modified model, as evidenced by Fig. 5.

Figure 6 shows the computed dependence of the velocity of the traveling stripe structure on the splay coupling coefficient λ for the modified model. The velocity decreases with the splay coupling strength and, in a reasonable approximation, the dependence of the velocity on $1/\lambda$ is linear inside the considered interval.

Numerical simulations of traveling domain structures have also been performed for the modified model. When flux is introduced ($\omega_0\neq0$), such domain structures move at a velocity proportional to ω_0 and no threshold for their motion could be detected (see Fig. 7). This indicates that the transition to translational motion for such patterns again represents
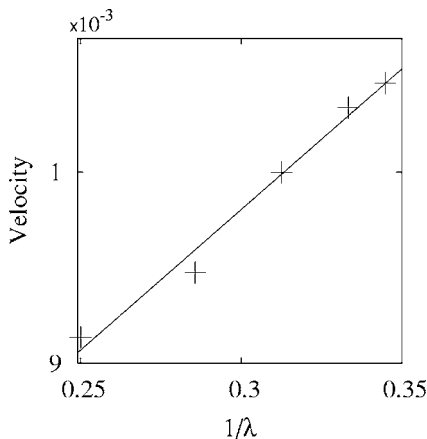
a linear response of the equilibrium patterns to the introduction of perturbations corresponding to the flow terms.

For stripe patterns, which spontaneously emerge as a result of the instability of the uniform state, the wavelength is fixed by the parameters of the system. In contrast, traveling domain structures may have different spatial periods, depending on the initial conditions. In that sense, they resemble periodic wave trains in excitable or oscillatory reaction-diffusion systems.

Computing the velocity V of the domain structures for different wave numbers $k=2\pi n/L$ with $n=1,2,3,...$, an interesting behavior is found. The dependence of V on k is nonmonotonous: it first increases when k grows and then begins to decrease (see Fig. 8).

V. NONEQUILIBRIUM 2D STRUCTURES

When leakage flux is introduced, wave activity develops in the equilibrium 2D structure shown in Fig. 3(a). The lines, which can be interpreted as domain boundaries, begin to move in the orthogonal direction. Additionally, short line segments decorating such boundaries are also running along them. As a result, complicated patterns displayed in Fig. 9 become established. In Fig. 9(a), corresponding to a smaller flux ($\omega=0.005$), the curved domain boundaries are seen to

FIG. 6. Velocity dependence of a traveling stripe pattern on $1/\lambda$ for Eqs. (5)–(7) with $c_0=0.2$, $\nu=0.1$, $g=1$, and $\omega_0=0.001$.
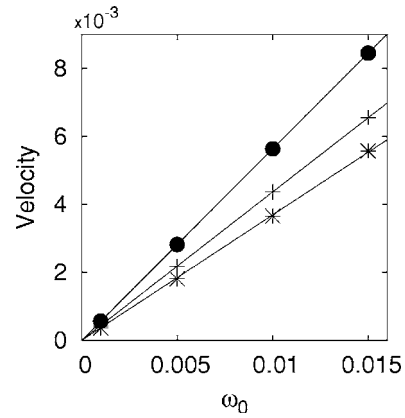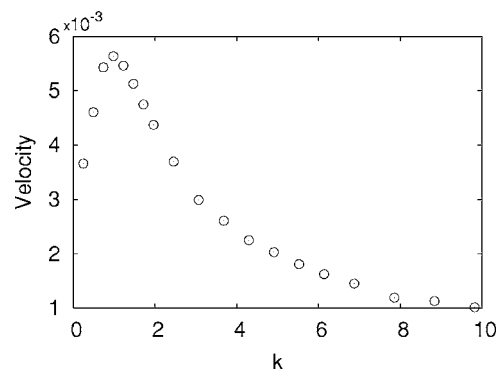

FIG. 8. Velocity of a traveling domain pattern plotted as a function of gradient k in initial azimuthal angle as $\phi(x)=kx$ with $\omega_0=0.01$, for Eqs. (5)–(7) for $c_0=0.1$, $\nu=0.1$, $g=1$, and $\lambda=4$.
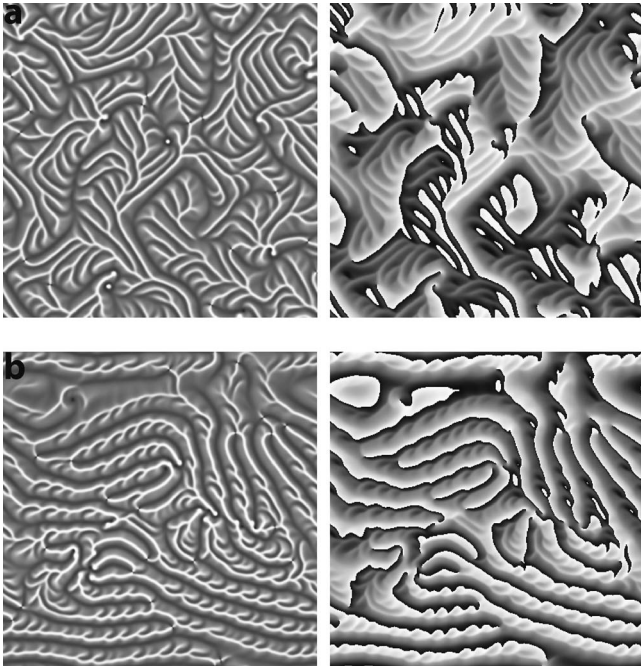
FIG. 9. Distributions of concentration (left panels) and azimuthal angle (right panels) in self-organized wave patterns obtained starting from random initial conditions for systems with the parameters $c_0=0.1$, $\lambda=4.0$, $\nu=10$, $g=10$, and $L=600$. The precession frequency ω is constant: (a) $\omega=0.005$ and (b) $\omega=0.01$. The concentration is displayed in gray scale with the darker color corresponding to lower concentration values.

form rotating spirals. For the higher fluxes [Fig. 9(b), $\omega=0.01$], the characteristic wavelength of the traveling domain pattern becomes shorter. At the same time, however, relatively large regions develop where oscillations are close to uniform. These regions are generating concentric waves that propagate away from them.

The structures shown in Figs. 3 and 9 correspond to a situation far from the critical point for the spontaneous formation of stripes in the medium (we have there $\lambda=4$ and $\lambda_{cr}=3.33\ldots$). The properties of the structures undergo a significant change as the splay coupling strength λ is decreased. An example of a nonequilibrium wave pattern for $\lambda=3.4$, $\omega=0.015$, and the same other parameters is shown in Fig. 10.
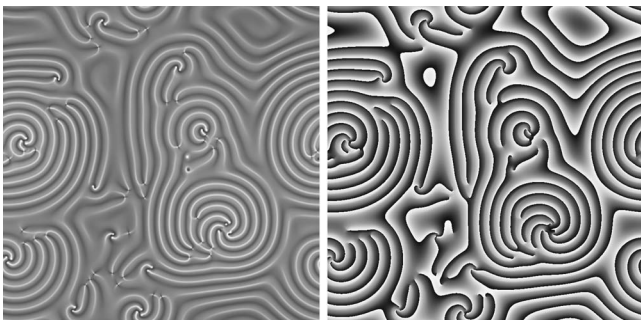

FIG. 10. Distributions of concentration (left panel) and azimuthal angle (right panel) in self-organized wave patterns obtained starting from random initial conditions for systems with the parameters $\lambda=3.4$, $\nu=0.01$, $g=1$, and $L=1600$. The frequency $\omega=0.015$ is constant and $c_0=0.1$. The concentration is displayed in gray scale with the darker color corresponding to lower concentration values.

Now, the stripe decorations of domain boundaries are not present. The pattern consists of the regions occupied by densely coiled waves that are slowly traveling into the direction toward their rotation centers (so that the spirals are inwardly rotating). In the central regions of such dense wave patterns, several orientational defects are visible. In the remaining parts of the medium, free from the dense wave patterns, oscillations are more uniform. These parts are repeatedly producing concentric waves that spread outwards into the dense wave regions which, therefore, look like "sinks" for the generated waves.

In our previous publication, the dense inwardly rotating structures were qualitatively interpreted as formed by the stripes.[19] This interpretation, as we see it now, was not correct. The examination of angle dependence in traveling waves in such patterns reveals that the azimuthal angle ϕ undergoes a complete rotation when each next wave is propagating. For a traveling stripe pattern, however, only periodic modulation of the angle around a certain equilibrium orientation is possible. Therefore, the observed traveling waves should rather be interpreted as formed by traveling domain structures. As seen in Fig. 8, the velocity of a traveling domain structure depends nonmonotonously on the wavelength. This may lead to modulational instabilities of waves. A detailed analysis of the nonlinear mechanisms responsible for the formation of the observed complex wave patterns will be performed in a separate publication.

The formation of spatiotemporal patterns in the considered system is accompanied by redistribution of chiral molecules.[19] Their concentration becomes increased in narrow spatial regions corresponding to domain boundaries. Additionally, there is also a large-scale gradual variation of the concentration in the medium. The concentration gets depleted in the areas occupied by the "target patterns" which are sending waves into the dense wave regions. This effect becomes strong for high leakage fluxes. In the simulation presented in Fig. 11(a), where the model with constant precession frequency is used, the central region becomes almost void with respect to the chiral molecules. Obviously, this result is not realistic. Indeed, only the response of the chiral molecules to the leakage flow brings the system away from thermal equilibrium and induces orientation precession. If the chiral molecules are practically absent in a large region, no precession should take place there. In such situations, the modified version of the model should rather be used, where the precession frequency is proportional to the local concentration of chiral molecules, $\omega=\omega_0(c/c_0)$. Numerical simulations using this modified model show that, for the same flux intensity (i.e., for ω_0 having the same values as ω in the simulation with the original model) and identical other parameters, concentration depletion in the central region remains moderate [see Fig. 11(b)].

So far, spatiotemporal pattern formation at low concentrations ($c_0=0.1$) of chiral molecules has been discussed. In the experiments, concentration of such molecules could not be made high, because the Langmuir monolayer was undergoing then a transition to a "frozen" solid state (Y. Tabe, private communication). This effect, involving breakdown of translational symmetry in the system, is absent in the consid-
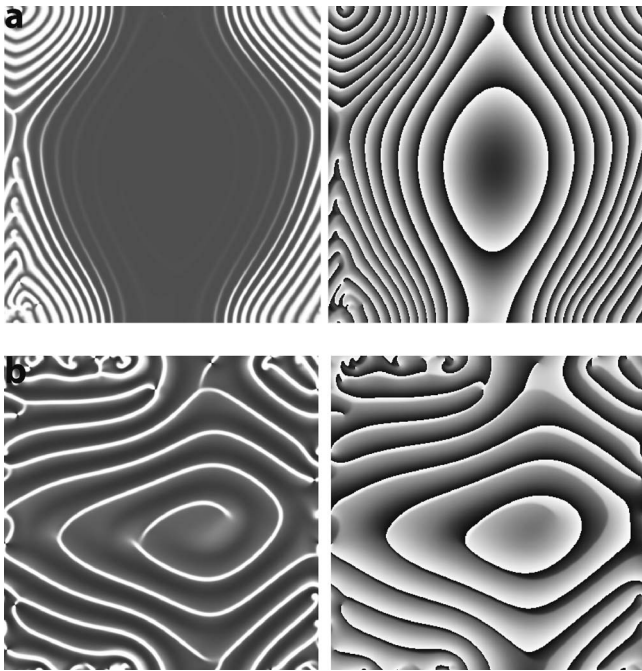
FIG. 11. Distributions of concentration (left panels) and azimuthal angle (right panels) in self-organized wave patterns obtained starting from random initial conditions for systems with the parameters $\lambda=3.4$, $\nu=0.01$, $g=1$, $L=200$, and $c_0=0.1$. (a) The frequency $\omega=0.015$ is constant. (b) The frequency is proportional to concentration: $\omega=\omega_0(c/c_0)$ with $\omega_0=0.015$. The concentration is displayed in gray scale with the darker color corresponding to lower concentration values.

ered simple model. Therefore, properties of nonequilibrium patterns at high concentrations of chiral molecules can be theoretically discussed.

The original model with constant precession frequency ω is invariant with respect to a change $c \rightarrow 1-c$ and $\lambda \rightarrow -\lambda$. The sign of the splay coupling coefficient λ is not important for pattern formation and, therefore, this symmetry implies that the variable c can be interpreted either as the concentration of chiral or nonchiral molecules in the system. Hence, for a high concentration of chiral molecules, $c_0=0.9$, and the same other parameters, one expects the same spatiotemporal patterns as for $c_0=0.1$, with the only difference being that c
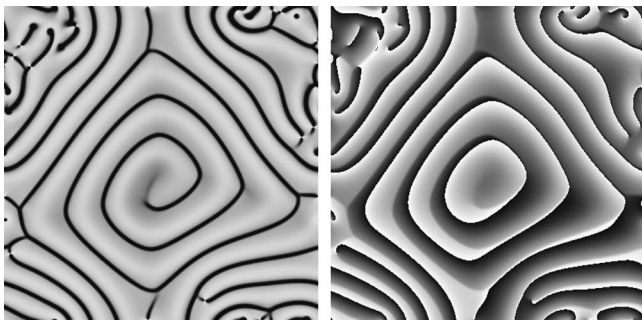

FIG. 12. Distributions of concentration (left panels) and azimuthal angle (right panels) in self-organized wave patterns obtained starting from random initial conditions for systems with the parameters $\lambda=3.4$, $\nu=0.01$, $g=1$, $L=200$, and $c_0=0.9$. The frequency is proportional to concentration: $\omega=\omega_0(c/c_0)$ with $\omega_0=0.015$. The concentration is displayed in gray scale with the darker color corresponding to lower concentration values.

should then represent the concentration on the remaining, nonchiral molecules.[19]

This invariance is absent in the modified model with $\omega=\omega_0(c/c_0)$. Qualitatively, however, numerical simulations of this model at high initial concentration $c_0=0.9$ of chiral molecules yield similar results (see Fig. 12). Now, local concentration of chiral molecules becomes sharply decreased in the spatial regions corresponding to traveling domain boundaries, where local azimuthal orientation undergoes a rapid change. On a large scale, concentration of chiral molecules is enhanced then in the "target pattern" areas that are sending concentric waves.

VI. CONCLUSIONS

Our investigations of the model, including splay coupling between the orientation field and local concentration of chiral molecules, show that leakage flows may lead to the formation of complex wave patterns in such nonequilibrium soft matter systems. Boundary conditions do not play a significant role in these phenomena. To emphasize this, our numerical simulations were performed using periodic boundary conditions, where no physical boundaries of a medium are introduced. The model successfully reproduces several characteristic features of the experimental patterns.[12] Particularly, the spontaneous formation of "target" wave sources, sending waves that propagate into the periphery regions, densely filled with the waves, should be pointed out. Further experiments are needed to test other predictions of the theory, involving spatial redistribution of chiral molecules inside the Langmuir monolayer.

The considered model is based on several simplifications. The most important of them is that the Langmuir monolayer is treated as being incompressible, so that its local density remains constant. Only the local composition of the monolayer, i.e., the local fraction of chiral molecules, is allowed to vary in the model. In reality, the monolayer density may also vary and, in principle, splay coupling between the molecular orientation and the density field should also be taken in account. Another simplification is that hydrodynamic effects have been neglected in the theoretical description. Such hydrodynamic effects should become especially important when experiments are performed for free-standing films, instead of the Langmuir monolayers.

Biomembranes are closely related to Langmuir monolayers and we expect that similar results should hold, under appropriate conditions, also for the membranes including a fraction of chiral molecules. The leakage flow in such systems is created by a gradient of concentration of small molecules or ions that leak through the membrane. This flow may bring the membrane to nonequilibrium conditions, giving rise to traveling waves and complex self-organized wave patterns. Importantly, chiral molecules (and, possibly, some passive inclusions) can then be transported and spatially redistributed in a membrane as a result of wave propagation.

using a parallel supercomputer in the Yukawa Institute for Theoretical Physics at Kyoto University. One of us (T.S.) acknowledges financial support through a grant for young scientists from the Ministry of Education, Culture, Sports, Science and Technology in Japan.

[1] A. S. Mikhailov and E. Ertl, Science **267**, 476 (1995).
[2] B. Hess and A. S. Mikhailov, Science **264**, 223 (1994).
[3] A. S. Mikhailov and B. Hess, J. Biol. Phys. **28**, 655 (2002).
[4] M. Hildebrand, A. S. Mikhailov, and G. Ertl, Phys. Rev. Lett. **76**, 1162 (1996).
[5] Y. De Decker and A. S. Mikhailov, J. Phys. Chem. B **108**, 14759 (2004).
[6] V. M. Kaganer, H. Möhwald, and P. Dutta, Rev. Mod. Phys. **71**, 779 (1999).
[7] Y. Tabe and H. Yokoyama, Langmuir **11**, 4609 (1995).
[8] Y. Tabe, T. Yamamoto, and H. Yokoyama, New J. Phys. **5**, 65 (2003).
[9] R. Reigada, F. Sagues, and A. S. Mikhailov, Phys. Rev. Lett. **89**, 038301 (2002).
[10] R. Reigada, A. S. Mikhailov, and F. Sagues, Phys. Rev. E **69**, 041103 (2004).
[11] T. Okuzono, Y. Tabe, and H. Yokoyama, Phys. Rev. E **69**, 050701 (2004).
[12] Y. Tabe and H. Yokoyama, Nat. Mater. **2**, 806 (2003).
[13] A. M. Zhabotinsky and A. N. Zaikin, Nature (London) **225**, 535 (1970).
[14] S. Ramaswamy, J. Toner, and J. Prost, Phys. Rev. Lett. **84**, 3494 (2000).
[15] H.-Y. Chen, Phys. Rev. Lett. **92**, 168101 (2004).
[16] P. Lenz, J.-F. Joanny, F. Jülicher, and J. Prost, Phys. Rev. Lett. **91**, 108104 (2003).
[17] R. Voituriez, J. F. Joanny, and J. Prost, Phys. Rev. Lett. **96**, 028102 (2006).
[18] Y. Tsori and P.-G. de Gennes, Eur. Phys. J. E **14**, 91 (2004).
[19] T. Shibata and A. S. Mikhailov, Europhys. Lett. **73**, 436 (2006).
[20] J. V. Selinger, Z. G. Wang, R. F. Bruinsma, and C. M. Knobler, Phys. Rev. Lett. **70**, 1139 (1993).
[21] J. V. Selinger and R. L. Selinger, Phys. Rev. E **51**, R860 (1995).
[22] R. D. Kamien and J. V. Selinger, J. Phys.: Condens. Matter **13**, R1 (2001).
[23] T. Ohyama, A. E. Jacobs, and D. Mukamel, Phys. Rev. E **53**, 2595 (1996).
[24] If a monolayer consists of chiral molecules, the splay term generally is $\Lambda c \nabla \cdot \mathbf{n}'$, where $\mathbf{n}'$ is obtained from $\mathbf{n}$ by rotation by some fixed angle α. Since all other terms in the free energy are, however, invariant with respect to such rotation, it is not important for pattern formation and we put here $\alpha = 0$.